ParisTech
INSTITUT DES SCIENCES ET TECHNOLOGIES
PARIS INSTITUTE OF TECHNOLOGY

MINES ParisTech

École doctorale nº 364 : Sciences Fondamentales et Appliquées

Doctorat ParisTech

T H È S E

pour obtenir le grade de docteur délivré par

l'École Nationale Supérieure des Mines de Paris

Spécialité doctorale "Science et Génie des Matériaux"

présentée et soutenue publiquement par

Ali SAAD

le xx juin 2015

NUMERICAL MODELLING OF MACROSEGREGATION INDUCED BY SOLIDIFICATION SHRINKAGE IN A LEVEL SET APPROACH

Directeurs de thèse: **Michel BELLET**
Charles-André GANDIN

Jury

M. Blablabla,	Professeur, MINES ParisTech	Rapporteur
M. Blablabla,	Professeur, Arts Et Métiers ParisTech	Rapporteur
M. Blablabla,	Chargé de recherche, ENS Cachan	Examinateur
M. Blablabla,	Danseuse, en freelance	Examinateur
M. Blablabla,	Ingénieur, MIT	Examinateur

MINES ParisTech
Centre de Mise en Forme des Matériaux (CEMEF)
UMR CNRS 7635, F-06904 Sophia Antipolis, France

THESE

Contents

1 General Introduction **1**

1.1 Solidification notions . . . 3
1.1.1 Solute partitioning . . . 3
1.1.2 Dendritic growth . . . 4
1.1.3 Mush permeability . . . 5
1.2 Macrosegregation . . . 6
1.2.1 Liquid thermosolutal convection . . . 7
1.2.2 Solidification shrinkage . . . 8
1.2.3 Movement of equiaxed grains . . . 8
1.2.4 Solid deformation . . . 8
1.3 Other defects . . . 8
1.4 Industrial Worries . . . 10
1.5 Project context and objectives . . . 11
1.5.1 Context . . . 11
1.5.2 Ojectives and outline . . . 12

2 Modelling Review **15**

2.1 Modelling macrosegreation . . . 16
2.1.1 Macroscopic solidification model: monodomain . . . 17
2.2 Eulerian and Lagrangian motion description . . . 23
2.2.1 Overview . . . 23
2.2.2 Interface capturing . . . 25
2.3 Solidification models with level set . . . 25
2.4 The level set method . . . 26
2.4.1 Diffuse interface . . . 26
2.4.2 Mixing Laws . . . 28
2.5 Interface motion . . . 30
2.5.1 Level set transport . . . 31
2.5.2 Level set regularisation . . . 32

3 Energy balance with thermodynamic tabulations **37**
3.1 State of the art . . . 38
3.2 Thermodynamic considerations . . . 38
3.2.1 Volume averaging . . . 38
3.2.2 The temperature-enthalpy relationship . . . 39
3.2.3 Tabulation of properties . . . 40
3.3 Numerical method . . . 43
3.3.1 Enthalpy-based approach . . . 45
3.3.2 Temperature-based approach . . . 45
3.3.3 Convergence . . . 46
3.4 Validation . . . 47
3.4.1 Pure diffusion . . . 47
3.4.2 Convection and diffusion . . . 50
3.5 Application: multicomponent alloy solidification . . . 53
3.5.1 Tabulations . . . 55
3.5.2 Discussion . . . 56

4 Macrosegregation with liquid metal motion **61**
4.1 Introduction . . . 62
4.2 Formulation stability . . . 62
4.2.1 Stable mixed finite elements . . . 62
4.2.2 Variational multiscale (VMS) . . . 63
4.3 VMS solver . . . 64
4.3.1 Variational formulation . . . 64
4.3.2 CFL condition . . . 64
4.3.3 Integration order . . . 64
4.4 Application to multicomponent alloys . . . 64
4.4.1 Results . . . 66
4.5 Macroscopic prediction of channel segregates . . . 67
4.5.1 Introduction . . . 67
4.5.2 Experimental work . . . 70
4.5.3 Macroscopic scale simulations . . . 70
4.6 Meso-Macro prediction of channel segregates . . . 77
4.6.1 Numerical method . . . 77
4.6.2 Configuration . . . 79
4.6.3 Effect of vertical temperature gradient . . . 82
4.6.4 Effect of cooling rate . . . 84
4.6.5 Effect of lateral temperature gradient . . . 86
4.6.6 Mono-grain freckles . . . 88

5 Macrosegregation with solidification shrinkage **89**
5.1 Solidification shrinkage 90
5.2 Choice of interface tracking 90
5.3 Multidomain formalism 92
5.3.1 Assumptions 93
5.4 Metal FE model 94
5.4.1 Mass and momentum conservation 94
5.4.2 Energy conservation 96
5.4.3 Species conservation 98
5.5 FE model: Air 100
5.5.1 Mass and momentum conservation 101
5.5.2 Energy conservation 101
5.5.3 Species conservation 101
5.6 FE monolithic model 101
5.6.1 Permeability mixing 101
5.6.2 Model equations 102
5.6.3 Interface treatment 102
5.7 Shrinkage without macrosegregation 104
5.7.1 Al-7wt% Si 105
5.7.2 Pb-3wt% Sn 105
5.8 Shrinkage with macrosegregation 105
5.8.1 Al-7wt% Si 105
5.8.2 Pb-3wt% Sn 105

Bibliography **107**

Acronym	Standing for
ALE	Arbitrary Lagrangian-Eulerian
BTR	Brittleness temperature range
CAFD	Cellular Automata Finite Difference
CAFE	Cellular Automata Finite Element
CBB	Circumventing Babuška-Brezzi
CCEMLCC	Chill Cooling for the Electro-Magnetic Levitator in relation with Continuous Casting of steel
CEMEF	Center for Material Forming
CSF	Continuum Surface Force
DLR	Deutsches Zentrum für Luft- und Raumfahrt
EML	Electromagnetic levitation
ESA	European Space Agency
FEM	Finite Element Method
GMAW	Gas Metal Arc Welding
ISS	International Space Station
IWT	Institut für Werkstofftechnik
LHS	Left Hand Side
LSM	Level set method
MAC	Marker-and-cell
PF	Phase field
RHS	Right Hand Side
RUB	Ruhr Universität Bochum
RVE	Representative Elementary Volume
SBB	Satisfying Babuška-Brezzi
SCPG	Shock Capturing Petrov-Galerkin
SUPG	Streamline Upwind Petrov-Galerkin
VMS	Variational MultiScale
VOF	Volume Of Fluid

Chapter 5

Macrosegregation with solidification shrinkage

Contents

5.1 Solidification shrinkage 90
5.2 Choice of interface tracking 90
5.3 Multidomain formalism 92
5.3.1 Assumptions 93
5.4 Metal FE model 94
5.4.1 Mass and momentum conservation 94
5.4.2 Energy conservation 96
5.4.3 Species conservation 98
5.5 FE model: Air 100
5.5.1 Mass and momentum conservation 101
5.5.2 Energy conservation 101
5.5.3 Species conservation 101
5.6 FE monolithic model 101
5.6.1 Permeability mixing 101
5.6.2 Model equations 102
5.6.3 Interface treatment 102
5.7 Shrinkage without macrosegregation 104
5.7.1 Al-7wt% Si 105
5.7.2 Pb-3wt% Sn 105
5.8 Shrinkage with macrosegregation 105
5.8.1 Al-7wt% Si 105
5.8.2 Pb-3wt% Sn 105

5.1 Solidification shrinkage

Solidification shrinkage is, by definition, the effect of relative density change between the liquid and solid phases. In general, it results in a progressive volume change during solidification, until the phase change has finished. The four stages in figs. 5.1a to 5.1d depict the volume change with respect to solidification time. First, at the level of the first solid crust, near the local solidus temperature, the solid forms with a density greater than the liquid's. The subsequent volume decrease creates voids with a negative pressure, forcing the fluid to be sucked in the direction of the volume change (cf. fig. 5.1b). As a direct result of the inward feeding flow, the ingot surface tends to gradually deform in the feeding direction, forming the so-called *shrinkage pipe*. Since the mass of the alloy and its chemical species is conserved, a density difference between the phases ($\rho^l < \rho^s \implies \frac{\rho^l}{\rho^s} < 1$) eventually leads to a different overall volume ($V^s < V^l$) once solidification is complete, as confirm the following equations:

$$\rho^l V^l = \rho^s V^s \tag{5.1a}$$

$$V^s = \frac{\rho^l}{\rho^s} V^l \tag{5.1b}$$

Solidification shrinkage is not the only factor responsible for volume decrease. Thermal shrinkage in both solid and liquid phases, as well as solutal shrinkage in the liquid phase are also common causes in a casting process. However, thermal shrinkage is very important to apprehend as temperature decrease in steel casting usually exceeds a 1000 °C, causing substantial density variations.

5.2 Choice of interface tracking

In chapter 2, several methods of interface tracking/capturing methods were presented along with their similarities and differences. In the case of solidification shrinkage, the metal-air interface can be tracked with any method from the previously mentioned. However, several reasons motivate us to settle on the level set method. First, the easiest solution is testing a method which already exists in *CimLib* library. The level set method was implemented by HERE as a framework for monolithic resolution. Since this work, the method has been extensively used and improved in several projects mainly for multiphase flows, which is the main competence of the Computational Fluids LXXXX group at CEMEF. Another motivation is the compatibility between *CimLib* and *Thercast*®, where the latter is the final destination of the code developed during for the Ph.D. thesis. In its recent versions, *Thercast*®handles laminar and turbulent ingot filling where the level set method is used to capture the free surface of the molten metal. Aside from the practical motivations, some technical aspects of the level set method make it very attractive to apply it macroscopic surface tracking

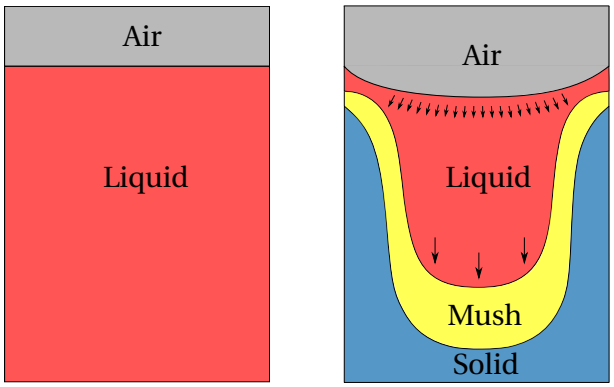

(a) Initial state **(b)** Early intermediate state

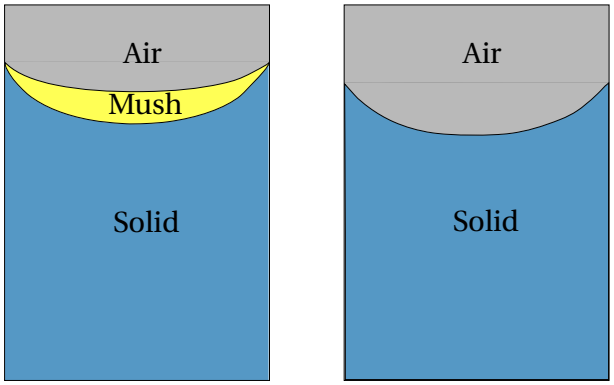

(c) Late intermediate state **(d)** Final state

Fig. 5.1 – Schematic of the main cooling stages of an ingot against side and bottom mould walls (not shown)

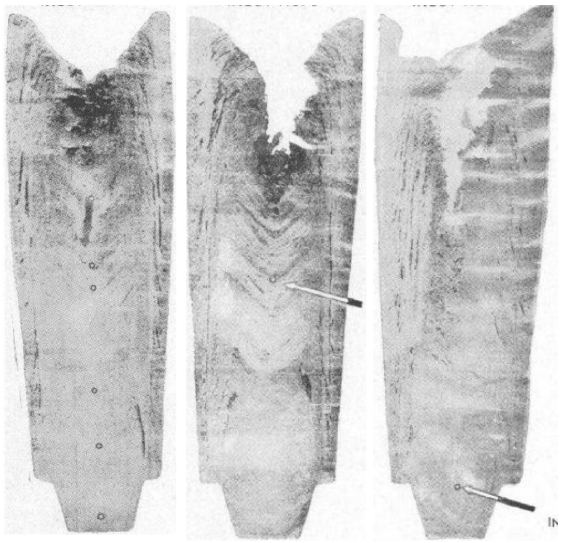

Fig. 5.2 – Sulphur prints of three ingots showing pipe formation at the top as a result of solidification shrinkage with various ingot inclination during casting [Onodera et al. 1959].

(in contrast to microscopic interface tracking, for instance the solid-liquid interface), such as topological properties that are readily available (e.g. curvature) and accurate position compared to volume-based methods like VOF.

5.3 Multidomain formalism

In the previous chapters, we considered in our simulations the metal as a saturated mixture of solid and liquid during solidification. It means that no gas phase may appear during the process, and this this chapter. The reason is we chose to describe our model in Eulerian description, for which we have considered a fixed grid to discretise the averaged conservation equations governing the phase change between the liquid and solid phases. Furthermore, with the introduction of shrinkage, an increase in global density means that a gas phase should enter the domain to replace the shrunk volume. At this point, several interfaces may be distinguished: liquid-solid (l-s), liquid-air (l-a) and solid-air (s-a), where we defined 2 phases (l and s) belonging to the "Metal" domain denoted M, while the "Air" domain, denoted A, is made up of a unique phase, (a), with the same name. As a standard for this formalism, we consider that uppercase letters are used for domains, while lowercase letters are used for phases.

The main idea behind the multidomain formalism, is to go from the classic conservations equations introduced by volume averaging in chapter 2, in the context of a solidifying two-phase system to generalise it by taking into account a third gas phase, such as:

$$V^l + V^s + V^a = V_\mathrm{E} \tag{5.2}$$

$$g^l + g^s + g^a = 1 \tag{5.3}$$

while keeping a physical integrity with the former monodomain model. Then, one is free to choose a suitable numerical method to track the interfaces between the several phases. In our applications, we are particularly interested in keeping an indirect representation of the l-s interface (dotted line in fig. 5.3) using the volume averaging theory, while employing a different method to track the l-a and s-a interfaces (dashed lines in fig. 5.3) with the level set method. This allows switching to the latter method in a physically representative manner.

In this context, each domain can be seen as a material having a physical interface with the other domains. As a consequence of our interpretation, the gas phase should not exist in the metal, which may naturally occur if the thermodynamic conditions are in favour of nucleating and growing a new phase, or in the case of a gas that was trapped inside mould grooves.

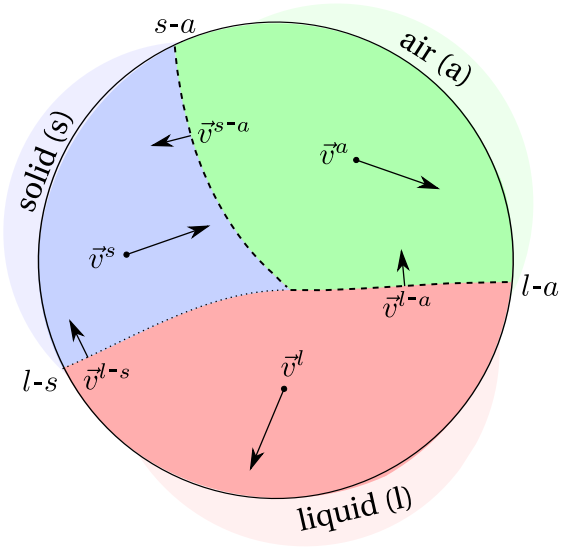

Fig. 5.3 – Schematic of a representative volume element containing 3 phases with distinct velocities, separated by 3 interfaces. The dotted line is the indirectly tracked solid-liquid interface while the other dashed lines, air-liquid and air-solid interfaces, are directly tracked.

5.3.1 Assumptions

Each phase in the system has its own velocity, $\vec{v}^{l}$, $\vec{v}^{s}$ and $\vec{v}^{a}$, while the respective interfaces l-s, l-a and s-a have different and independent velocities, represented by $\vec{v}^{l\text{-}s}$, $\vec{v}^{l\text{-}a}$ and $\vec{v}^{s\text{-}a}$. Note that the solid-liquid interface velocity was denoted $\vec{v}^{*}$ in the previous chapters as no more than two phases were considered. The first major assumption is that the solid phase, once formed from the liquid, is fixed and rigid. It means that no subsequent deformation may occur and therefore $\vec{v}^{s\text{-}a}$ reduces to vector zero. Moreover, we use the already introduced volume averaging principles to write locally for any quantity ψ:

$$\langle\psi\rangle = \langle\psi^{l}\rangle + \langle\psi^{s}\rangle + \langle\psi^{a}\rangle \tag{5.4a}$$

$$= g^{l}\psi^{l} + g^{s}\psi^{s} + g^{a}\psi^{a} \tag{5.4b}$$

where volume fractions, g^{ϕ}, for each phase ϕ were used. Rappaz et al. [2003] define the volume fraction by writing a general expression inside the representative volume V_{E}:

$$g^{\phi} = \frac{1}{V_{\mathrm{E}}}\int_{V_{\mathrm{E}}} \chi^{\phi}(x,t)\,\mathrm{d}\Omega \tag{5.5}$$

where the integrated quantity is an indicator (or presence) function relative to phase ϕ, which defines the volume of this phase in the system, Ω^{ϕ}, as follows:

$$\chi^{\phi}(x,t) = \begin{cases} 1 & \text{if } x \in \Omega^{\phi} \\ 0 & \text{otherwise} \end{cases} \tag{5.6}$$

Any phenomenon that may displace an interface, whether by phase change or a phase motion, is mathematically translated by variations of the presence function, i.e. spatial and temporal derivatives of the phase fraction. If we consider the liquid phase, these variations are given by:

$$\frac{\partial \langle \psi^l \rangle}{\partial t} = \langle \frac{\partial \psi^l}{\partial t} \rangle + \frac{1}{V_{\mathrm{E}}} \int_{l-a} \psi^l \vec{v}_n^{\,l\text{-}a} \, \mathrm{d}\Gamma + \frac{1}{V_{\mathrm{E}}} \int_{l-s} \psi^l \vec{v}_n^{\,l\text{-}s} \, \mathrm{d}\Gamma \tag{5.7}$$

$$\vec{\nabla} \langle \psi^l \rangle = \langle \vec{\nabla} \psi^l \rangle - \vec{n}^{\,l\text{-}s} \delta \left(x - x^{l\text{-}s} \right) \tag{5.8}$$

link with LS transport equation by looking into [Rappaz et al. 2003] p. 113 where the heaviside is the same as the indicator function.

5.4 Metal FE model

In this section, we start from a the monodomain finite element model presented in section 2.1.1 relevant to metal only, then present the essential assumptions and formulations that allow predicting solidification shrinkage in a Eulerian context.

5.4.1 Mass and momentum conservation

The metal domain consists of two phases, solid and liquid, which have unequal densities that vary with temperature. However, as we consider in the current project that the solid is static, then $\vec{v^s} = \vec{0}$, hence only the liquid's density may vary while the solid has a constant density. With these assumptions, one may write:

$$\frac{\partial \langle \rho \rangle}{\partial t}^{M} + \nabla \cdot \langle \rho \vec{v} \rangle^{M} = 0 \tag{5.9}$$

$$\tag{5.10}$$

Formulation

The mass balance equation averaged over the two phases, is expanded taking into account the aforementioned assumptions.

$$\frac{\partial \langle \rho \rangle}{\partial t} + \nabla \cdot \langle \rho \vec{v} \rangle = 0 \tag{5.11a}$$

$$\frac{\partial}{\partial t}\left(g^l \rho^l + g^s \rho^s\right) + \nabla \cdot \left(g^l \rho^l \vec{v}^l\right) = 0 \tag{5.11b}$$

$$g^l \cancel{\frac{\partial \rho^l}{\partial t}} + \rho^l \frac{\partial g^l}{\partial t} + g^s \cancel{\frac{\partial \rho^s}{\partial t}} + \rho^s \frac{\partial g^s}{\partial t} + \rho^l \nabla \cdot \left(g^l \vec{v}^l\right) + g^l \vec{v}^l \cdot \cancel{\vec{\nabla} \rho^l} = 0 \tag{5.11c}$$

$$\left(\rho^l - \rho^s\right) \frac{\partial g^l}{\partial t} + \rho^l \nabla \cdot \left(g^l \vec{v}^l\right) = 0 \tag{5.11d}$$

$$\boxed{\nabla \cdot \left(g^l \vec{v}^l\right) = \nabla \cdot \langle \vec{v}^l \rangle = \frac{\rho^l - \rho^s}{\rho^l} \frac{\partial g^s}{\partial t}} \tag{5.12}$$

With the assumptions of static solid phase and constant unequal phase densities, the average mass balance states that the divergence of the liquid velocity is proportional to the solidification rate, by a factor of density change, which results in a relative volume change. Equation (5.12) explains the flow due to shrinkage. In metallic alloys, the solid density is usually greater than the liquid density, therefore the first term in the RHS is negative. As for the second term, if we neglect remelting, then it'll be positive in the solidifying areas of the alloy. A negative divergence term in these areas, means that a liquid feeding is necessary to compensate for the density difference, hence acting as a flow driving force in the melt. In the case of constant densities, we can easily deduce that the divergence term is null, and therefore no flow is induced by solidification. Furthermore, additional terms should appear in the other conservation equations, balancing the volume change in the heat and species transport. When the metal's density was considered constant during solidification, the assumption of an incompressible system made it possible to use the Boussinesq approximation. However, in the case of solidification shrinkage, the average density $\langle \rho \rangle = g^s \rho^s + g^l \rho^l$ varies, since ρ^s and ρ^l are not equal. Naturally, these phase densities would depend on temperature and possibly on the phase composition. Therefore, the incrompressibility condition may not be true. In such case, the earlier given system eq. (2.41) is reformulated without

any reference value for density:

$$\begin{cases} \rho^l \left(\dfrac{\partial \langle \vec{v}^l \rangle}{\partial t} + \dfrac{1}{g^l} \vec{\nabla} \cdot \left(\langle \vec{v}^l \rangle \times \langle \vec{v}^l \rangle \right) \right) = \\ \quad - g^l \vec{\nabla} p^l - 2\mu^l \vec{\nabla} \cdot \left(\overline{\overline{\nabla}} \langle \vec{v}^l \rangle + \overline{\overline{\nabla^{\mathrm{t}}}} \langle \vec{v}^l \rangle \right) - g^l \mu^l \mathbb{K}^{-1} \langle \vec{v}^l \rangle + g^l \rho^l \vec{g} \\ \\ \nabla \cdot \langle \vec{v}^l \rangle = \dfrac{\rho^l - \rho^s}{\rho^l} \dfrac{\partial g^s}{\partial t} \end{cases} \tag{5.13}$$

5.4.2 Energy conservation

We have seen the averaged energy conservation equation in the case of two phases: a solid phase and an incompressible liquid phase. However, with the incorporation of the shrinkage effect, new terms should appear in the advective-diffusive heat transfer equation.

Assumptions

- The thermal conductivity is constant for both phases: $\langle \kappa \rangle = \langle \kappa^s \rangle = \langle \kappa^l \rangle = \kappa$
- Consequence of the static solid phase: $\langle \rho h \vec{v} \rangle = g^l \rho^l h^l \vec{v}^l + \cancel{g^s \rho^s h^s \vec{v}^s} = g^l \rho^l h^l \vec{v}^l$
- The system's enthalpy may thermodynamically evolve with pressure, knowing that $h = e + \frac{p}{\rho}$, where e is the internal energy and p is the pressure. It infers that the heat transport equation may contain a contribution attributed to volume compression/expansion:

  $$\frac{\partial p}{\partial t} + \nabla \cdot (p \vec{v}) = \frac{\partial p}{\partial t} + p \nabla \cdot \vec{v} + \vec{v} \cdot \vec{\nabla} p \tag{5.14}$$

  In the literature, this contribution has been always neglected, even when accounting for solidification shrinkage, owing to the small variations of pressure.

- The heat generated by mechanical deformation, $\mathbb{S} : \dot{\varepsilon}$, is neglected

Formulation

The unknowns in the energy conservation are the average volumetric enthalpy $\langle \rho h \rangle$ and temperature T.The energy conservation equation writes:

$$\frac{\partial \langle \rho h \rangle}{\partial t} + \nabla \cdot \langle \rho h \vec{v} \rangle = \nabla \cdot \left(\langle \kappa \rangle \vec{\nabla} T \right) \tag{5.15a}$$

$$\frac{\partial \langle \rho h \rangle}{\partial t} + \nabla \cdot \left(g^l \rho^l h^l \vec{v}^l \right) = \nabla \cdot \left(\kappa \vec{\nabla} T \right) \tag{5.15b}$$

$$\frac{\partial \langle \rho h \rangle}{\partial t} + \rho^l h^l \nabla \cdot \langle \vec{v}^l \rangle + \langle \vec{v}^l \rangle \cdot \vec{\nabla} \left(\rho^l h^l \right) = \nabla \cdot \left(\kappa \vec{\nabla} T \right) \tag{5.15c}$$

$$\frac{\partial \langle \rho h \rangle}{\partial t} + \cancel{\rho^l} h^l \frac{\rho^l - \rho^s}{\cancel{\rho^l}} \frac{\partial g^s}{\partial t} + \langle \vec{v}^l \rangle \cdot \vec{\nabla} \left(\rho^l h^l \right) = \nabla \cdot \left(\kappa \vec{\nabla} T \right) \tag{5.15d}$$

$$\frac{\partial \langle \rho h \rangle}{\partial t} + \left(\rho^l - \rho^s \right) h^l \frac{\partial g^s}{\partial t} + \langle \vec{v}^l \rangle \cdot \vec{\nabla} \left(\rho^l h^l \right) = \nabla \cdot \left(\kappa \vec{\nabla} T \right) \tag{5.15e}$$

$$\boxed{\frac{\partial \langle \rho h \rangle}{\partial t} + \rho^l \langle \vec{v}^l \rangle \cdot \vec{\nabla} h^l = \nabla \cdot \left(\kappa \vec{\nabla} T \right) + \left(\rho^s - \rho^l \right) h^l \frac{\partial g^s}{\partial t}} \tag{5.16}$$

In order to keep things simple, the term "enthalpy" will refer henceforth to "volume enthalpy", otherwise, we will explicitly use the term "mass enthalpy". It is important to understand the meaning of the terms in equation (5.16). The first term in the left-hand side is the temporal change in the system's average enthalpy, i.e. a temporal change in the volume enthalpy of any of the phases in the course of solidification. The second LHS term is a dot product between the superficial liquid velocity and the the gradient of the liquid's enthalpy. Since phase densities are constant in our case, the gradient term reduces to the liquid's mass enthalpy. If we consider a representative volume element (RVE) in the liquid phase, far from the mushy zone, we can stipulate:

$$\vec{\nabla} h^l = C_p^l \vec{\nabla} T \tag{5.17}$$

assuming that the phase mass specific heat, C_p^l, is constant. Therefore, the liquid enthalpy is advected in the case where the velocity vector is not orthogonal to the temperatre gradient. The advection reaches its maximum when the two vectors have the same direction. Consider, for instance, a filled ingot with a cooling flux applied to its bottom surface. If the density variation with temperature were to be neglected, then the sole mechanical driving force in the melt is the density jump at the solid-liquid interface ahead of the mushy zone. The temperature gradient in such a case is vertical upward, while the velocity vector is in the opposite direction. The advective term writes:

$$\rho^l \langle \vec{v}^l \rangle \cdot \vec{\nabla} h^l = -\rho^l C_p^l \| \langle \vec{v}^l \rangle \| \| \vec{\nabla} T \| \tag{5.18}$$

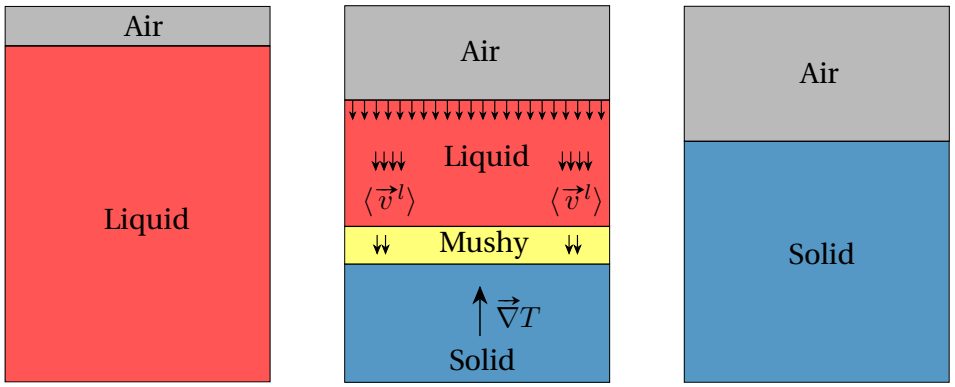

(a) Initial state **(b)** Solidification onset **(c)** Final state

Fig. 5.4 – Effect of one-dimensional shrinkage flow on a solidifying ingot

We see that the second LHS term in equation (5.16) acts as a heat source at the interface between the the phases, in this particular solidification scenario. Another heat power (of unit Wm^{-3}) adds to the system in the mushy zone, that is the second term in the RHS of the same equation. This term is proportional to the solidification rate. Finally, the first RHS term accounts for thermal diffusion within the phases.
It should be emphasized that the assumption of a constant specific heat in the liquid in equation (5.17) applies when no macrosegregation occurs. Nonetheless, when the latter is considered, the phases specific and latent heats become highly dependent on the local average composition. It then advisable to use the thermodynamic tabulation approach, where the enthalpies are directly tabulated as functions of temperature and intrinsic phase compositions.

5.4.3 Species conservation

The last conservation principle is applied to the chemical species or solutes. This principle allows predicting macrosegregation when applied to a solidification system, along with the mass, momentum and energy balances. However, the conservation equation should be reformulated in the case of a melt flow driven by shrinkage.

Assumptions

- The alloy is binary, i.e. it is composed from one solute, and hence the notation of the average composition without a solute index: $\langle w \rangle$ for the mass composition and $\langle \rho w \rangle$ for the volume composition
- The solid fration is determined assuming complete mixing in both phases, hence the lever rule is applied. The solidification path in the current approach is tabulated using thermodynamic data at equilibrium

- The macroscopic solute diffusion coefficient D^s in the solid phase is neglected in the mass diffusive flux term.

- The solid phase is fixed and rigid, therefore $\langle \rho w \vec{v} \rangle = g^l \rho^l \langle w \rangle^l \vec{v}^l + \cancel{g^s \rho^s \langle w \rangle^s \vec{v}^s} = g^l \rho^l \langle w \rangle^l \vec{v}^l$

Formulation

The species conservation is pretty similar the energy conservation formulated in the previous section. For a binary alloy, we write:

$$\frac{\partial \langle \rho w \rangle}{\partial t} + \nabla \cdot \langle \rho w \vec{v} \rangle - \nabla \cdot \left(\langle D^l \rangle \vec{\nabla} \left(\rho^l \langle w \rangle^l \right) \right) = 0 \tag{5.19a}$$

$$\langle \rho \rangle \frac{\partial \langle w \rangle}{\partial t} + \langle w \rangle \frac{\partial \langle \rho \rangle}{\partial t} + \nabla \cdot \left(g^l \rho^l \langle w \rangle^l \vec{v}^l \right) - \nabla \cdot \left(g^l D^l \vec{\nabla} \left(\rho^l \langle w \rangle^l \right) \right) = 0 \tag{5.19b}$$

$$\begin{aligned} &\langle \rho \rangle \frac{\partial \langle w \rangle}{\partial t} + \langle w \rangle \frac{\partial \langle \rho \rangle}{\partial t} + \left(\rho^l \langle w \rangle^l \right) \nabla \cdot \langle \vec{v}^l \rangle + \langle \vec{v}^l \rangle \cdot \vec{\nabla} \left(\rho^l \langle w \rangle^l \right) \\ &- \nabla \cdot \left(g^l D^l \vec{\nabla} \left(\rho^l \langle w \rangle^l \right) \right) = 0 \end{aligned} \tag{5.19c}$$

The mass balance gives the following relations:

$$\frac{\partial \langle \rho \rangle}{\partial t} + \nabla \cdot \langle \rho \vec{v} \rangle = 0 \tag{5.20a}$$

$$\frac{\partial \langle \rho \rangle}{\partial t} + \nabla \cdot \left(g^l \rho^l \vec{v}^l \right) = 0 \qquad (\rho^l \text{ is constant}) \tag{5.20b}$$

$$\nabla \cdot \langle \vec{v}^l \rangle = -\frac{1}{\rho^l} \frac{\partial \langle \rho \rangle}{\partial t} \tag{5.20c}$$

If we use the result of eq. (5.20c) in eq. (5.19c), then we get the following equation:

$$\langle \rho \rangle \frac{\partial \langle w \rangle}{\partial t} + \langle w \rangle \frac{\partial \langle \rho \rangle}{\partial t} = \langle w \rangle^l \frac{\partial \langle \rho \rangle}{\partial t} - \langle \vec{v}^l \rangle \cdot \vec{\nabla} \left(\rho^l \langle w \rangle^l \right) + \nabla \cdot \left(g^l D^l \vec{\nabla} \left(\rho^l \langle w \rangle^l \right) \right) \tag{5.21}$$

Applying Voller-Prakash [Voller et al. 1989] variable splitting, the system ends up with only one variable, which is the average composition $\langle w \rangle$. The splitting is done as follows:

$$\langle w \rangle^l = \left(\langle w \rangle^l \right)^t + \langle w \rangle - \langle w \rangle^t \tag{5.22}$$

where the superscript t refers to the previous time step. The chemical species conservation writes:

$$\begin{aligned}
&\langle\rho\rangle\frac{\partial\langle w\rangle}{\partial t} + \cancel{\langle w\rangle\frac{\partial\langle\rho\rangle}{\partial t}} = \\
&\cancel{\langle w\rangle\frac{\partial\langle\rho\rangle}{\partial t}} - \rho^l\langle\vec{v}^l\rangle\cdot\vec{\nabla}\langle w\rangle + \nabla\cdot\left(g^l\rho^l D^l\nabla\langle w\rangle\right) \\
&+ \frac{\partial\langle\rho\rangle}{\partial t}\left[\left(\langle w\rangle^l\right)^t - \langle w\rangle^t\right] - \rho^l\langle\vec{v}^l\rangle\cdot\vec{\nabla}\left(\langle w\rangle^t - \left(\langle w\rangle^l\right)^t\right) \\
&+ \nabla\cdot\left[g^l\rho^l D^l\vec{\nabla}\left(\left(\langle w\rangle^l\right)^t - \langle w\rangle^t\right)\right]
\end{aligned} \tag{5.23a}$$

$$\begin{aligned}
&\langle\rho\rangle\frac{\partial\langle w\rangle}{\partial t} + \rho^l\langle\vec{v}^l\rangle\cdot\vec{\nabla}\langle w\rangle - \nabla\cdot\left(g^l\rho^l D^l\nabla\langle w\rangle\right) = \\
&- \frac{\partial\langle\rho\rangle}{\partial t}\left[\langle w\rangle^t - \left(\langle w\rangle^l\right)^t\right] + \rho^l\langle\vec{v}^l\rangle\cdot\vec{\nabla}\left(\langle w\rangle^t - \left(\langle w\rangle^l\right)^t\right) \\
&- \nabla\cdot\left[g^l\rho^l D^l\vec{\nabla}\left(\langle w\rangle^t - \left(\langle w\rangle^l\right)^t\right)\right]
\end{aligned} \tag{5.23b}$$

$$\begin{aligned}
&\langle\rho\rangle\frac{\partial\langle w\rangle}{\partial t} + \rho^l\langle\vec{v}^l\rangle\cdot\vec{\nabla}\langle w\rangle - \nabla\cdot\left(g^l\rho^l D^l\nabla\langle w\rangle\right) = \\
&- \frac{\partial\langle\rho\rangle}{\partial t}\left[\langle w\rangle^t - \left(\langle w\rangle^l\right)^t\right] \\
&+ \rho^l\langle\vec{v}^l\rangle\cdot\vec{\nabla}\left(\langle w\rangle^t - \left(\langle w\rangle^l\right)^t\right) - \nabla\cdot\left[g^l\rho^l D^l\vec{\nabla}\left(\langle w\rangle^t - \left(\langle w\rangle^l\right)^t\right)\right]
\end{aligned} \tag{5.24}$$

It is noted that eq. (5.24) is valid only if both densities ρ^l and ρ^s are constant but have different values. Since density changes are incorporated in this equation, inverse segregation following solidification shrinkage is predicted. For the case where macrosegregation is solely due to fluid flow generated by natural or forced convection, i.e. no shrinkage occurs whether due to thermal-solutal contraction or phase change, the overall volume remains constant, hence density is constant. In this situation, $\rho^s = \rho^l = \langle\rho\rangle$ and the term $\partial\langle\rho\rangle/\partial t$ therefore vanishes. After dividing both sides by $\langle\rho\rangle = \rho^l$, eq. (5.24) reduces to:

$$\begin{aligned}
&\frac{\partial\langle w\rangle}{\partial t} + \langle\vec{v}^l\rangle\cdot\vec{\nabla}\langle w\rangle - \nabla\cdot\left(g^l D^l\nabla\langle w\rangle\right) \\
&= \langle\vec{v}^l\rangle\cdot\vec{\nabla}\left(\langle w\rangle^t - \left(\langle w\rangle^l\right)^t\right) - \nabla\cdot\left[g^l D^l\vec{\nabla}\left(\langle w\rangle^t - \left(\langle w\rangle^l\right)^t\right)\right]
\end{aligned} \tag{5.25}$$

5.5 FE model: Air

Conservation equations for the air are close to those derived for the metal as a fluid, with the exception of some points:

- air is a fluid that will not undergo any phase change, hence constant heat diffusivity;
- species conservation is irrelevant in the air as it is considered a pure material;
- unlike metal, air is considered incompressible at any time.

5.5.1 Mass and momentum conservation

5.5.2 Energy conservation

5.5.3 Species conservation

The composition of alloying elements is crucial quantity to predict in this work. Nevertheless, such prediction is only relevant in the metallic alloy, even if the air is also made up of other chemical species (nitrogen, oxygen ...). For this obvious reason, the species conservation equation should not be solved in the air, but that of course is contradictory to the monolithic resolution. The consequence is that we should compute the conservation of chemical species in the air and the metal, but limit as much as possible the influence of the former, in a way to prevent a "numerical" solute exchange between these domains. To do so, the computed air velocity will not be used here for advection, but rather use a zero-velocity vector instead. As diffusion is also another transport mechanism that may alter the conservation principle, a very low macroscopic solute diffusion coefficient can be used, as long as its order of magnitude is at most a thousand times less than that in the melt, $D^A \lll D^l$. The low artificial diffusion in the air may slightly violate the wanted no-exchange condition at the air-liquid interface, but it is known that suppressing the diffusion term in the air would result in a stiff partial differential equation that may be difficult to solve.

$$\frac{\partial}{\partial t}\left(\rho^A \langle w \rangle^A\right) + \cancel{\nabla \cdot \left(\rho^A \langle w \rangle^A \langle \vec{v}^a \rangle\right)} - \nabla \cdot \left(\rho^A D^A \vec{\nabla} \langle w \rangle^A\right) = 0 \tag{5.26}$$

$$\boxed{\frac{\partial}{\partial t}\left(\rho^A \langle w \rangle^A\right) - \nabla \cdot \left(\rho^A D^A \vec{\nabla} \langle w \rangle^A\right) = 0} \tag{5.27}$$

5.6 FE monolithic model

The monolithic model combines all conservations equations in metal and air in a unique set of equations to be solved on a fixed mesh. This can be accomplished by using the Heaviside function (defined in section 2.4.1) relative to each domain.

5.6.1 Permeability mixing

How to mix liquid fraction, best using harmonic or arithmetic, in order to replicate the effect the of non slip condition at top for example

Put the python plots from the presentations in "TEXUS monolithic"
Put video animations of PSEUDO SMACS 2D without and with LS ???

5.6.2 Model equations

Rewrite air-metal monolithic conservation equations using mixture laws.

5.6.3 Interface treatment

The level set method, like any other interface tracking/capturing method, needs defining a convenient way of coupling the velocity field on the one hand, which is the solution provided by solving momentum conservation equations, with the interface position on the other hand. The question is "how does the velocity field transport the interface?". The answer is potentially one of two possibilities: classical coupling or modified coupling. In the next subsections, we discuss the technical details of each approach and the hurdles that come with it.

Classical coupling

A "classical" coupling comes in the sense of "unmodified" coupling. This approach consists of taking the output of the fluid mechanics solver, then feed it as raw input to level set transport solver. The physical translation would be that the interface motion is dictated by the fluids flow in its vicinity. No treatment whatsoever is done between the two mentioned steps. While conservation principles are best satisfied with this approach, the latter yields some drawbacks, preventing its application in a generic way. For instance, the free liquid surface is not necessarily horizontal at all times and that can lead to the wrong shrinkage profile when solidification is complete.

present the example of unstable interface when the ratio between fluids properties became greater than some value+discussion

Modified coupling

In contrast to a classic coupling, here we attempt to modify the velocity field before feeding to the transport solver. The main motivation for considering this approach is the lack of stability that we observed whenever the mechanical properties of the fluids were different by several orders of magnitude. The algorithm should simultaneously fulfil these requirements:

- support high ratios of fluids density with close viscosities by preserving an non-oscillating interface,
- maintain a horizontal level at the free surface of the melt,
- follow shrinking metal surface profile in solidfying regions,

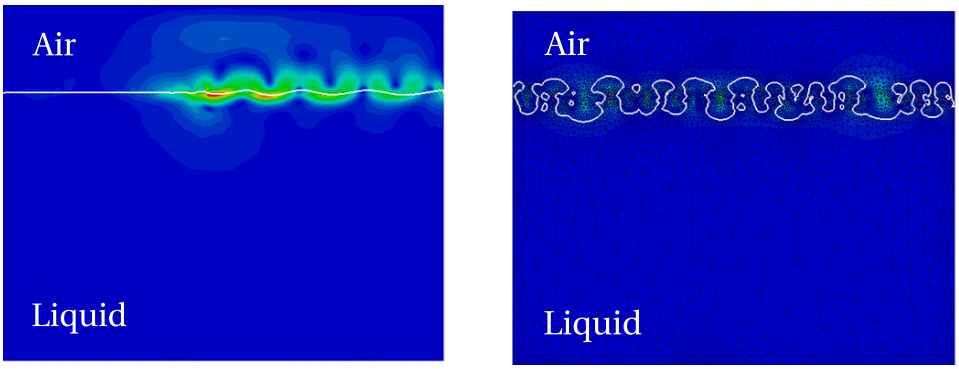

(a) At a certain time increment (without mesh)

(b) Another time increment (with mesh)

Fig. 5.5 – Interface destabilisation under the effect of high properties ratio across the interface.

- satisfy the mass conservation principle, essentially in the metal.

We want to process the original transport velocity by imposing a uniform motion (speed and direction) at the nodes of the free surface, and at the same time, be able to follow the pipe formation at the surface as a result of solidification shrinkage, as shown in fig. 5.6.

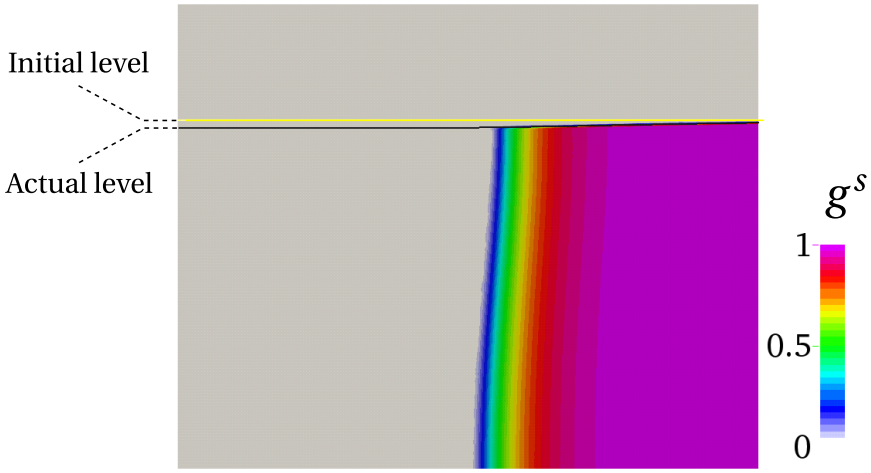

Fig. 5.6 – Snapshot of a solidifying ingot by a cooling flux from the side. The profile of the actual surface changes in solid and mushy regions to adapt the new density while staying perfectly horizontal in the liquid phase.

How to transport level set using velocity from momentum conservation DIRECTLY or AVERAGED PER ELEMENTS, show examples of instability/stability when using false/nominal air properties
Validation of LS transport: perform test case simulation of buoyancy driven air droplet in water by 2005Nagrath that I also have seen in Shyamprasad's masters report). => I didnt notice: what time step δt did they use ?

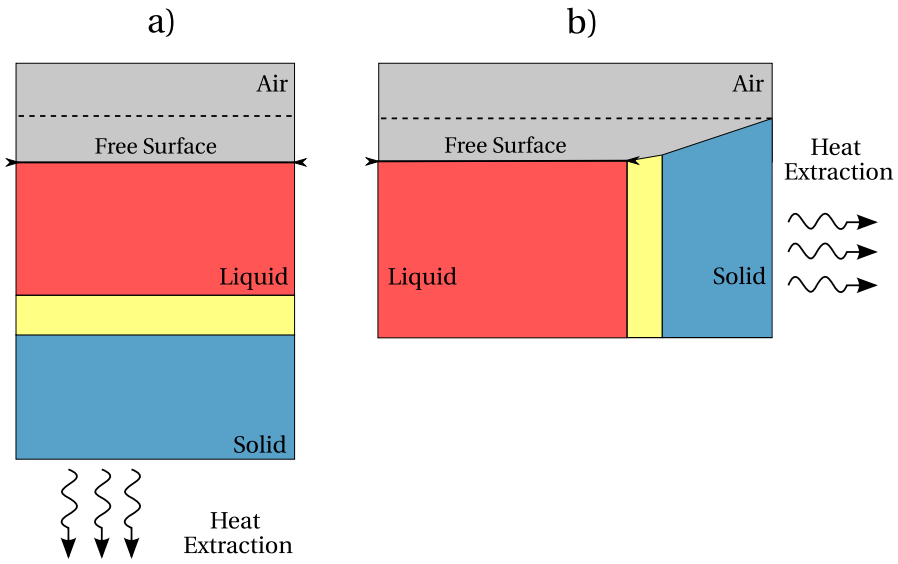

Fig. 5.7 – Treatment of liquid free surface in a) bottom and b) side heat extraction configurations. The dashed line represents the initial level of the free liquid surface.

The general idea is read the velocity around the interface up to a certain thickness, which may be the same thickness as the diffuse interface defined in section 2.4.1, then compute a volumetric average from all the elements in the thickness. This average is then given to the transport solver, which will apply the same magnitude and direction to transport the interface. However, as we only need the transport velocity to be uniform within the "100% liquid" elements, it should not be the case for the other elements that belong either to the mushy zone or the solid region, where shrinkage is taking place. Therefore, depending on the heat extraction configuration, two scenarios are possible. If heat extraction is far from the interface, i.e. there is not direct contact as in fig. 5.7a, the surface area remains unchanged at any time, hence all the elements around the interface are "100% liquid". This happens when a bottom cooling is applied to the ingot. In contrast, if a side cooling is applied as shown in fig. 5.7b, the surface area of the interface will be reduced over time as a consequence of the solid front progression. In this case, the average transport velocity should be computed only from the elements belonging to the free surface. The remaining part of the interface which belongs to partial or full solid regions, is transported with Navier-Stokes output, which should be some orders of magnitude less than the velocity imposed at the free surface, as a result of a decreasing permeability.

5.7 Shrinkage without macrosegregation

Explain how the flow and heat transfer in the air are not important
Give the strong form equations to be solved OR simply refer the previous section where

the model was defined
Initial and boundary conditions for energy and momentum: Initially we have liquid and air at rest.

5.7.1 Al-7wt% Si

Present pseudo 1D case with results + discussion

5.7.2 Pb-3wt% Sn

Present 2D and 3D case with results + discussion

5.8 Shrinkage with macrosegregation

Explain how the flow and heat transfer in the air are not important
Give the strong form equations to be solved OR simply refer the previous section where the model was defined
Initial and boundary conditions for energy and momentum: Initially we have liquid and air at rest.

5.8.1 Al-7wt% Si

Present pseudo 1D case with results + discussion

5.8.2 Pb-3wt% Sn

Present 2D and 3D case with results + discussion

Bibliography

[Onodera et al. 1959]
Onodera, S. and Arakida, Y. (1959). "Effect of Gravity on the Macro-Segregation of Larger Steel Ingots", pp. 358–368. URL: http://eprints.nmlindia.org/3079/1/358-368.PDF (cited on page 91).

[Rappaz et al. 2003]
Rappaz, M., Bellet, M., and Deville, M. (2003). *Numerical Modeling in Materials Science and Engineering*. Springer Series in Computational Mathematics. Springer Berlin Heidelberg (cited on pages 93, 94).

[Voller et al. 1989]
Voller, V. R., Brent, A. D., and Prakash, C. (1989). "The modelling of heat, mass and solute transport in solidification systems". *International Journal of Heat and Mass Transfer*, 32 (9), pp. 1719–1731. URL: http://www.sciencedirect.com/science/article/pii/0017931089900549 (cited on page 99).